Automatic Inspection of Epoxy Die-attach Process of a Semiconductor Chip

CATALIN GHEORGHE AMZA*
University Politehnica of Bucharest, 313 Spl. Independentei, 060042, Bucharest, Romania

This paper concerns with a method for automatic detection of voids as a result of epoxy die-attach process of a semiconductor chip to the package. A radiographic image is acquired from the inspected semiconductor chip and package and image processing techniques are employed in order to automatically compute the amount of epoxy die-attach voids.

Keywords: image processing, X-ray imaging, image segmentation, artificial intelligence

The purpose of die-attach or die-bonding is to provide a reliable attachment of the semiconductor chip to the package while meeting functionality requirements of the package as a whole. The idea behind it is the industry drive for smaller packages that will fit into portable consumer electronics such as cell phones, medical devices, portable computers, pagers, etc. Furthermore, while using faster and powerful chips, the thermal requirements are much more rigorous. The most used procedure is the epoxy die-attach due to its cost-effectiveness. The most encountered defect in the epoxy die-attach process is the void. Voids that appear between the chip and the package can shorten the life cycle of the chip and can also affect the chip's performance. Hence, inspection of the chip and package must be performed in order to meet quality requirements. Automation of such inspection process is a must in a modern manufacturing process, due to costs and time constraints. The inspection stage must be fast and reliable and needs to be performed in real time on the actual manufacturing line. One of the most used automatic inspection system in the industry is based on acquiring some sort of image of the inspected product and the consequent analysis of it [1, 2]. In case of epoxy die-attach, the most used image is the radiographic image (an X-ray image of the inspected chip and package is obtained by using an X-ray source and an image intensifier).

An automated inspection system of the epoxy die-attach process can provide a method to calculate precisely the amount of die-attach voids. By comparing the results with an accepted amount, one can reject or accept the final product, according to the inspection quality standards and requirements.

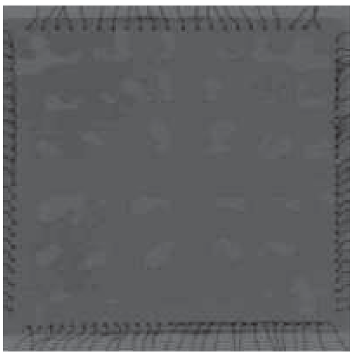

Fig. 1. X-ray image of chip with epoxy die-attach voids

The proposed automated system is depicted in figure 2.

A summary of the proposed inspection process is presented below [3]:

Step 1

- Acquire the X-ray image or images of the inspected product

Step 2

- Low-level image processing of the resulting image or images

a)X-ray image or images pre-processing

b)X-ray image segmentation

Step 3

- High-level detection of voids amount

Step 4

- Final product acceptance or rejectance

Experimental part

In the X-ray images taken, the raw information is in most of the cases presented in a way unsuitable for the human eye or for further image analysis techniques (poor contrast, presence of noise, etc.) [4], [5]. Therefore, methods for "improving" or enhancing the images were developed. The contrast of an image is given by the distribution of its grey levels or its pixel values. If this

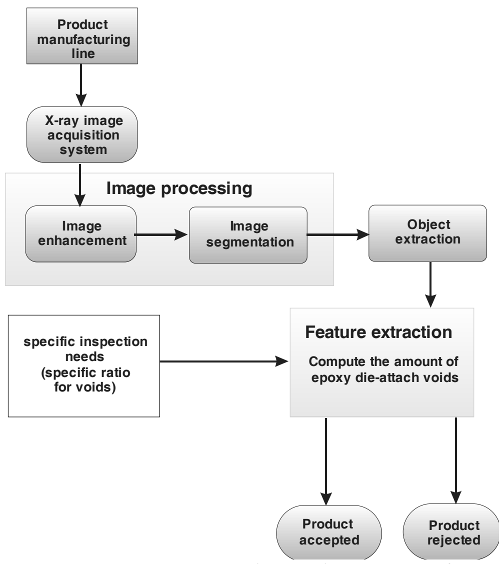

Fig. 2. The proposed automated inspection system of epoxy die-attach voids amount

* *email: amza_catalin@yahoo.com; Tel.: 021 402 95 41*

distribution is concentrated near a certain level, then the contrast is obviously low. On the other hand, when a wide range of grey levels are presented in the image, then the contrast is high. It is the main objective of image pre processing to improve images to appear suitable for the human eye [5]. Only after pre-processing, further automated computer based image analysis algorithms can be employed, since all are based on the knowledge gathered through human visual senses [6]. Furthermore, transmission over cables of video signals is often affected by the presence of electromagnetic fields, bad shielding of cables, etc. Consequently, noise can corrupt the resultant images. The noise pattern consists of strong, spike like components that can affect randomly the grey-value of one or more pixels, called impulse or salt-and-pepper noise. Methods used for noise removal are usually based upon spatial-domain techniques [7]. The pre-processing stage of the acquired X-ray image consists of applying a median filter. Contrast enhancement techniques from the spatial-domain are also employed [1]. The aim here is to have a resultant image that contains contours for the voids. The idea under lying edge detection is the computation of a local derivative operator. The first derivative of an edge modelled in this manner is 0 in all regions of constant grey level and constant during a grey-level transition. The first derivative of an image is called *gradient* and it is defined as follows:

$$G_{f(x,y)} = \frac{\partial f}{\partial x} + \frac{\partial f}{\partial y} \quad (1)$$

The computation of the *gradient* of an image consists in the determination of the partial derivatives at every pixel location *(x,y)*. A 3 by 3 mask (or convolution kernel) was used. The *Laplacian* edge enhancement technique produces sharper edge definition than most other techniques. Its main property is that it can highlight edges in all directions. The Laplacian of an image *f(x,y)* can be determined as follows:

$$L_{f(x,y)} = \frac{\partial^2 f}{\partial x^2} + \frac{\partial^2 f}{\partial y^2} \quad (2)$$

where

$$\frac{\partial^2 f}{\partial x^2} = f(x+1) - 2f(x) + f(x-1) \quad (3)$$

$$\frac{\partial^2 f}{\partial y^2} = f(y+1) - 2f(y) + f(y+1)$$

An approximation of the *Laplacian* can be derived as:

$$L_{f(x,y)} = -4f(x,y) + f(x+1,y) + f(x-1,y) + \\ + f(x,y+1) + f(x,y-1) \quad (4)$$

Sobel and *Prewitt* filters were also tested on the X-ray images. The difference with the *Laplacian* and *gradient* operators is that the X-ray images were analyzed for horizontal and vertical contour in two independent passes and then the results mathematically processed.

Figure 3 presents the results of pre-processing Step of the image depicted in figure 1.

Once pre-processing is completed, image segmentation techniques [8] are applied in order to partition the image into meaningful objects (voids and non-voids) for the consequent analysis.

A simple thresholding of the acquired X-ray image (segmentation into two classes) would provide a useless result for further image analysis techniques. To illustrate this, an Otsu-based [9] algorithm was implemented. The results are depicted in figure 4. When thresholding the

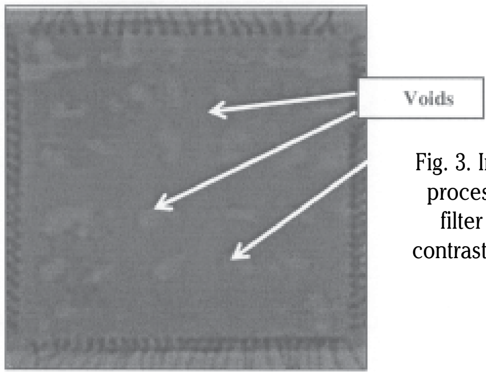

Fig. 3. Image after pre-processing (median filter applied and contrast enhancement)

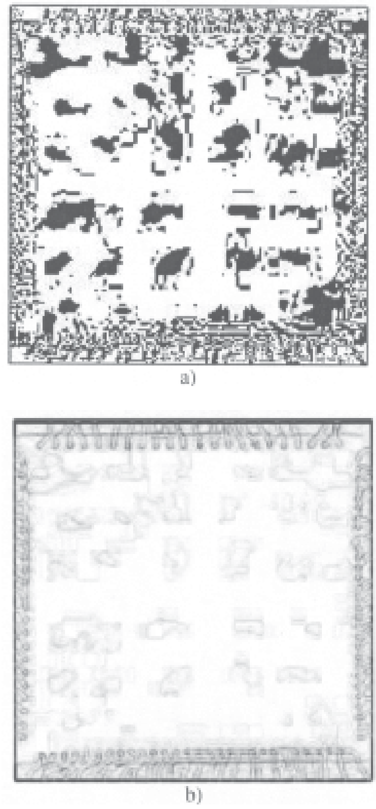

Fig. 4. Segmentation using a) Otsu's thresholding algorithm; b) Classical edge enhancement (Laplacian edge enhancement algorithm)

image, voids are merged with other parts of the background (fig. 4 a) and therefore, a correct extraction of important objects is not possible in this way. Therefore, multilevel thresholding techniques need to be employed to solve the segmentation problem [10]. Classical edge enhancement and detection techniques were also tested on the X-ray images [11]. *Sobel* and *Prewitt* filters were also tested on the X-ray images (fig. 5). The difference with the *Laplacian* and *gradient* operators is that the X-ray images were analysed for horizontal and vertical contour in two independent passes and then the results mathematically processed.

Classical methods of image segmentation applied to the acquired X-ray images with respect to an inspection system have proven to render results that are not very useful for further image analysis such as high-level detection (due to the merging between voids and the surrounding background). Since image segmentation output is the input to consequent image processing techniques, one wants that output to be of a high quality.

The segmentation process can also be seen as a constraint optimization and the consequent analysis can be viewed as a pattern recognition problem [12]. The constraints, in this case are based on the fact that objects extracted from the image needs to be homogenous and different from each other for instance. Thus, an

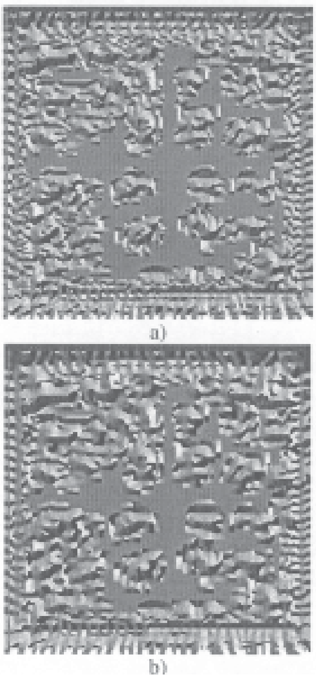

Fig. 5. Application of Sobel (a) and Prewitt (b) filter for classical edge detection

alternative approach to image segmentation was implemented by using a Hopfield Neural Network architecture (HNN) [13-15]. A general implementation of HNN to solve constraint optimisation problems is presented below, [17]:

i.determine the input representation in a way that the final solution is indicated by the output of the neurons;

ii. determine the cost function or the energy of the HNN. This should be in the form of a Lyapunov function [1];

iii.include constraints terms in the cost function of the HNN (in a Lyapunov form);

iv. differentiate the defined Energy function with respect of time in order to obtain the equations for the network' dynamics [4];

v. randomly choose the starting values for the HNN and start the updating algorithm;

vi. extract the solution from the equilibrum (stable) state of the HNN.

Once the segmentation process is completed, the method should be able to automatically compute the amount of epoxy die-attach voids. Thus, the computation is merely a process of counting the black and white pixels, and to compute a corresponding ratio. The resulting ratio is compared with a look-up table containing accepted ratios and a final decision is taken whether the chips is accepted or rejected.

For each segmentation level, a backtracking algorithm was designed and implemented for the object extraction and to compute each object size. It consists of a function that requires a starting point (pixel) of the current object to extract. Then, all pixels adjacent to the starting pixel are tested for similarity. If a pixel is found to be the same grey-level as the object, then it is marked respectively. Otherwise the process is stopped. The algorithm is called backtracking due to the fact that the function is called recursively within itself. The algorithm searches for neighbor pixels from right to left for instance and it continues to do so until a dead end is reached; then the function "backtracks" its way to the starting point and the process continues for considering pixels from left to right and so on.

When the function has marked all the pixels of an object, its size is computed. By summing all object sizes, one can compute the amount of epoxy die-attach voids from the inspected product. The algorithm is presented below.

Backtracking algoritm for epoxy die-attach voids computation determination

```
Func Object_extraction(starting point(x,y))
Begin
      if starting_point(x,y)
(does not belong to the object segmentation level) and (it was considered before)
then STOP
      else
//Pixel belongs to the object and it was not
//considered before
      Begin
      Increment Object_size;
      mark (x,y) as (already being considered);
//start and check the neighbouring pixels
             Object_extraction(x+1,y);
             Object_extraction(x-1,y);
             Object_extraction(x,y-1);
             Object_extraction(x,y+1);
                    end;
end;
```

The starting point of an object is obtained by scanning the segmented image line by line until the first pixel within the current segmentation level is found. That pixel is considered as being the starting point of a new and not considered object within the analysed class.

Results and discussions

The proposed method was applied to a number of 49 X-ray images. The images were simply segmented into 2, 3 and 4 classes and then the amount of voids was computed. A performance rate was computed as being the amount computed divided by the actual amount of voids computed manually. The average performance rates for the bank of images used are depicted in table 1.

Table 1
PERFORMANCE VERSUS NUMBER OF CLASSES FOR SEGMENTATION

Number of classes	Performance rate
2	78.3%
3	**92.3%**
4	86.4%

As one can guess, the performance rate highly depends on the actual segmentation result. One must find the optimum number of classes for the segmentation algorithm in order to make sure that the segmentation into two classes (fig. 6) will merge part of the voids with the background and that will mean that the amount of voids computed subsequently is less than the actual figure. Segmentation into four classes will lead to a highly

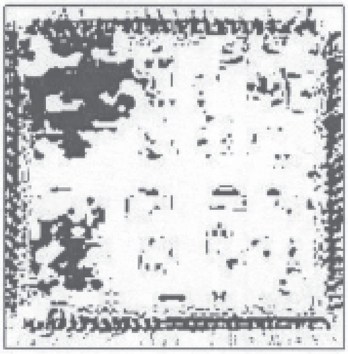

Fig. 6. HNN segmentation into two classes

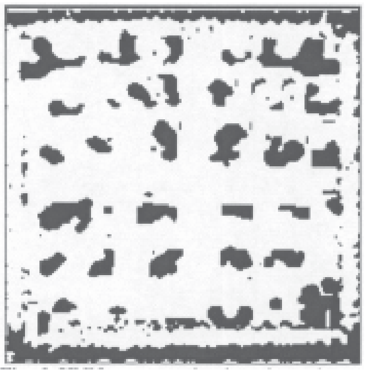

Fig. 7. HNN segmentation into three classes

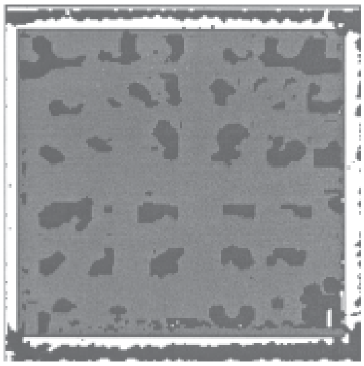

Fig. 8. Frame (area) for the computation of the amount of die-attach voids

fragmented segmented images, where parts of the background are to be considered voids. This leads to the computed amount of voids being higher than the real figure. Segmentation into three classes has proven experimentally to be the best case here (fig. 7). The margins of the chip that contains the connection pins are not taken into consideration when computing the amount of die-attach voids (outside the calculations rectangle depicted in figure 8.

Conclusions

This paper proposed a method for automatic inspection of epoxy die-attach. An X-ray image is acquired from the inspected chip and package and it is processed. The algorithm simply automatically computes the amount of voids in order to take a decision whether the product corresponds from the quality point of view (if the amount of voids is below certain threshold, the functionality of the package as a whole is maintained). The use of artificial intelligence technique such as the use of a Hopfield Neural Network for the image segmentation and the use of a backtracking algorithm in order to compute the amount of voids had proven the reliability of the proposed method. Further work concerns with decreasing the computational workload implied by the backtracking algorithm in order to make the proposed method suitable for real-time applications with very low response times. The number of classes for segmentation had been determined experimentally, for the type of images presented. However, further work is necessary in order to find a method for the automatic generation of the number of classes for the segmentation algorithm, based on the spatial and grey-level distribution information from the cluster of images used.

References

1.AMZA, C., G., Intelligent X-ray Imaging Inspection System for the Food Industry, PhD Thesis, De Montfort University, Leicester, United Kingdom, 2002

2.CONNOLLY, C., X-ray systems for security and industrial inspection, Sensor Review, Vol. 28 Iss: 3, p.194 – 198, 2008

3.AMZA, C.G., AMZA, G., CICIC, D.T., POPESCU D., Modern industrial foreign body detection systems, Proceedings of the 12th International Conference on Technology and Quality for Sustained Development, ISSN 1844-9158, pag. 11-20, 2012

4.KAUR M., KAUR J., Survey of contrast enhancement techniques based on histogram equalization, International Journal of advanced Computer Science and Applications (IJACSA), vol2, no.7, p.137-141, 2011

5.CHAABANI, A.C., BOUJELBEN, A., MAHFOUDHI, A., ABID, M. (2010). An Automatic-Pre-processing Method for Mammographic Images. International Journal of Digital Content Technology and its Applications, vol. 4, no. 3, pp.190-200

6.AMZA, C.G., TASCA, G., Segmentation of Industrial X-ray images, Proceedings of the 4th WSEAS International Conference on Computational Intelligence CI'10, Bucharest, Romania, 2010, p.54-59

7.KEHOE, A., Parker, G.A., An intelligent knowledge based approach for the automated radiographic inspection of castings, NDT&E International, vol. 25, no.1, p.23-36, 1992

8.AMZA, C.G., AMZA, G., Popescu D., Image segmentation for industrial quality inspection, rev. Fiability and Durability, Supplement no.1/2012, Ed. "Academica Brancusi", Targu Jiu, p.126-132, 2012

9.OTSU, N., A threshold selection method from grey-level histograms, IEEE Trans. On systems, man and Cybernetics, vol. SMC-9, no.1, p.62-66, 1979

10.Ch.HIMA BINDU, An Improved Medical Image Algorithm Using Otsu Method, International Journal of Recent Trends in Engineering, Vol 2, No. 3, November 2009

11.LEUNG, C.K., Lam, F.K., Maximum segmented image information thresholding, Graphical Models and Image Processing, vol.60, no.1, p. 57-76, 1998

12.CHEN, C., Statistical Pattern Recognition, Hayden, Washington, 1973

13.HOPFIELD J.J., Neurons with graded response have collective computational properties like those of two-state neurons, Biophysics: Proc.Natl.Acad.Sci., USA, vol.81, p.3088-3092, May, 1984

14.HOPFIELD, J.J., Neural networks and physical systems with emergent collective computational abilities, Proc. Natl.Acad.Sci., USA, vol.79, p.2554-2558, April, 1982

15.HOPFIELD, J.J., Tank, D.W., "Neural" Computation of Decisions in Optimisation Problems, Biol.Cybern., vol.52, p.141-152, 1985

16.CHANG, C.Y. (2003). Contextual Hopfield Neural Networks for Medical Image Edge Detection. 16th IPPR Conference on Computer Vision, Graphics and Image Processing (CVGIP), p.161-167

Manuscript received: 23.09.2014